J. Fluid Mech. (2007), *vol.* 593, *pp.* 463–473.
doi:10.1017/S0022112007008622 Printed in the United Kingdom

Laminar flow in a two-dimensional plane channel with local pressure-dependent crossflow

P. HALDENWANG

Modélisation et Simulation Numérique en Mécanique et Génie des Procédés (MSNM-GP),
UMR-CNRS 6181 – Universités d'Aix-Marseille – ECM
IMT/La Jetée – Technopôle de Château Gombert, 38, rue Frédéric
Joliot-Curie – 13451 Marseille Cedex 20, France

(Received 20 April 2007 and in revised form 10 September 2007)

Long ducts (or pipes) composed of transpiring (e.g. porous) walls are at the root of numerous industrial devices for species separation, as tangential filtration or membrane desalination. Similar configurations can also be involved in fluid supply systems, as irrigation or biological fluids in capillaries. A transverse leakage (or permeate flux), the strength of which is assumed to depend linearly on local pressure (as in Starling's law for capillary), takes place through permeable walls. All other dependences, as osmotic pressure or partial fouling due to polarization of species concentration, are neglected. To analyse this open problem we consider the simplest situation: the steady laminar flow in a two-dimensional channel composed of two symmetrical porous walls.

First, dimensional analysis helps us to determine the relevant parameters. We then revisit the Berman problem that considers a uniform crossflow (i.e. pressure-independent leakage). We expand the solution in a series of R_t, the transverse Reynolds number. We note this series has a rapid convergence in the considered range of R_t (i.e. $R_t \leqslant O(1)$). A particular method of variable separation then allows us to derive from the Navier–Stokes equations two new ordinary differential equations (ODE), which correspond to first and second orders in the development in R_t, whereas the zero order recovers the Regirer linear theory. Finally, both new ODEs are used to study the occurrence of two undesirable events in the filtration process: axial flow exhaustion (AFE) and crossflow reversal (CFR). This study is compared with a numerical approach.

1. Introduction

Species separation is the object of numerous industrial processes. Schematically, a permeable membrane supposed to retain the concerned species is used, and in a very popular set-up (tangential filtration) the membrane composes the wall of a duct. Then, the species remains in the carried (or axial) flow, while the purified fluid leaves the duct by crossing the membrane. In practice, those ducts are cylindrical pipes, but for the reasons discussed below the present analysis considers a two-dimensional channel composed of two identical homogeneous parallel walls, separated by spacing $2d$.

Modelling the strength of the flow that crosses the permeable walls is not a trivial task, because in principle it depends on different local quantities. We first have in mind the pressure difference between both sides of the wall. The crossflow should

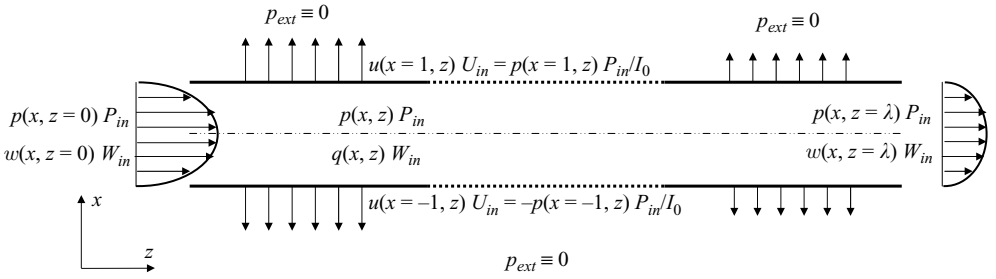

FIGURE 1. Sketch of steady two-dimensional channel flow with pressure-dependent suction at the walls.

also depend on species concentration through osmotic pressure. Another concept linked with species rejection at the permeable wall is the so-called polarization of concentration at the wall. The latter phenomenon can be so intense that the membrane filtration properties are strongly affected (see Bacchin, Aimar & Field (2006) for a review of those complex features). The problem addressed in the paper, however, focuses on the first dependence; hence $U_c(z)$, the velocity normal to the wall (i.e. the crossflow), depends linearly on the inner pressure at the membrane, denoted $P_c(z)$, while the outer pressure is assumed to be uniform, and chosen as the reference pressure (i.e. $P_{ext} = 0$). The relationship between normal velocity and local pressure is

$$U_c(z) = P_c(z)/I_0, \tag{1.1}$$

where I_0, the so-called wall resistance, is a uniform (constant) quantity. Note also that osmotic pressure is absent from (1.1), and in the rest of the paper the fluid is assumed pure, incompressible and with constant properties. Figure 1 summarizes the channel geometry and problem assumptions.

Even with these drastic simplifications, the resulting problem is considered open, although the state of the art contains of a very few partial solutions. Before discussing the state of the art, we must define an important non-dimensional parameter, the transverse Reynolds number, as

$$R_t \equiv d\rho_0 U_{c|in}/\mu_0 = d\rho_0 P_{c|in}/(\mu_0 I_0), \tag{1.2}$$

where ρ_0 and μ_0 denote fluid density and dynamic viscosity. Subscript zero reminds us the concerned quantity is uniform, '$_{|in}$' indicates that the data are those at channel entrance, and '$_c$' denotes a quantity relative to crossflow.

Berman (1953) gave an exact solution to a different problem: a channel with a uniform crossflow ($U_c(z) = U_{c|in}$) at the walls was considered. Now, for a particular value of R_t (denoted R_t^{iso}, with $R_t^{iso} \approx 1.3107$), inertial effects exactly compensate for viscous effects, in such a way that the flow remains isobaric along the whole channel wall (i.e. $P_c(z) = P_{c|in}$). Therefore, for this particular value of R_t, Berman provided us with the exact solution of our original problem.

Let us consider $R_t = 0$, another particular value of R_t. It is little known in the western literature that the solution for $R_t = 0$ was first published by Regirer (1960). This exact solution has been rediscovered independently several times since.

Galowin, Fletcher & DeSantis (1974) showed that inertial effects can dominate, and lead to a pressure increase due to suction at the walls. Although slightly inconsistent (as discussed below), their derivation permitted a relevant interpretation of their experimental observations.

The paper aims to bridge the gap between these theoretical approaches. Its base line is the Berman exact solution in a channel, although filtration in a tube is more relevant for standard applications. For the time being, it is preferable to develop a theory in the context of channel flow for the following reasons: (i) mathematical developments are easier in plane geometry; (ii) a Berman solution (labelled Type I in literature) continuously exists for all R_t in a channel (Robinson 1976); (iii) the stability of this solution is not called into question for $R_t \leqslant 6$ (Zaturska, Drazin & Banks 1988); (iv) a solution of Type I rapidly develops from parabolic inlet conditions if $R_t \leqslant 4$; more precisely, a relative error less than 5 % in pressure variation is introduced if inlet boundary conditions are of Poiseuille type instead of Berman type (Gupta & Levy 1976; see also Brady 1984).

2. Dimensional analysis and basic properties

As defined in § 1, our problem obviously depends on seven independent dimensional parameters: $\{d,\ \rho_0,\ \mu_0,\ I_0,\ L,\ P_{in},\ W_{in}\}$. The last three parameters are, respectively, the channel length, the inlet mean pressure and the inlet mean axial velocity. The application of dimensional analysis leads us to consider four independent numbers only; we shall define them after introducing the mathematical model and the following auxiliary quantities. We first define U_{in}, the order of magnitude of the transverse velocity, as $U_{in} = P_{in}/I_0$, while the dead-end length, denoted L_{de}, corresponds to $L_{de} = W_{in}d/U_{in}$. The latter length gives the distance from the inlet where axial flow exhaustion would occur, if the flow were isobaric.

Our study starts from the steady Navier–Stokes equations that govern the motion of a uniform property fluid in the domain $\Omega = \{-d < X < d\} \times \{0 < Z < L\}$. The equations read in dimensional form

$$\nabla\cdot\boldsymbol{V} = 0 \qquad \text{in} \quad \Omega, \tag{2.1}$$

$$(\boldsymbol{V}\cdot\nabla)\boldsymbol{V} = -\frac{1}{\rho_0}\nabla P + \frac{\mu_0}{\rho_0}\Delta\boldsymbol{V} \qquad \text{in} \quad \Omega, \tag{2.2}$$

together with the boundary conditions on the walls ($\boldsymbol{n}$ is the outer normal unit vector)

$$\boldsymbol{n}\cdot\boldsymbol{V}(X = \pm d, Z) = P(X = \pm d, Z)/I_0, \quad \boldsymbol{V} - (\boldsymbol{n}\cdot\boldsymbol{V}(X = \pm d, Z))\,\boldsymbol{n} = 0. \tag{2.3}$$

It is worth noting that we do not yet provide any boundary conditions at the inlet or outlet. We shall impose inlet conditions of the Berman type (see below). For the range of the standard parameters relative to filtration (i.e. $R_t \leqslant O(1)$), the results of § 5 indicate that Hagen–Poiseuille flow–taken as inlet conditions–does not produce important modifications. Let us now introduce the following non-dimensional unknowns and variables, used throughout the paper

$$u = \frac{U}{U_{in}}, \quad w = \frac{W}{W_{in}}, \quad p = \frac{P}{P_{in}}, \quad x = \frac{X}{d}, \quad z = \frac{Z}{L_{de}}. \tag{2.4}$$

Note that the choice retained here implies that the typical magnitude of all non-dimensional variables is expected to be one. On the other hand, the four independent numbers we have selected to characterize the problem are

$$R_t = \frac{\rho_0 U_{in} d}{\mu_0}, \quad \lambda = \frac{L}{L_{de}}, \quad \alpha = \left(\frac{\mu_0 I_0 W_{in}^2}{P_{in}^2 d}\right)^{1/2}, \quad \beta = \frac{\mu_0}{I_0 d}. \tag{2.5}$$

Number R_t, the transverse Reynolds number, compares inertial to viscous effects. Let us give more detail about this classic sentence. For reasons of symmetry, the

channel mid-line (i.e. the symmetry axis $x=0$) is a trajectory of the laminar flow (the inlet conditions being indeed symmetrical). Suppose the flow along this trajectory stops at L_{de}, the point of isobaric exhaustion. On the one hand, neglecting viscous effects and invoking the Bernoulli theorem, we observe a pressure increase of the order of $0.5\rho_0 W_{in}^2$. On the other hand, supposing the flow to be close to a Hagen–Poiseuille flow, we estimate the viscous pressure drop at $-3\mu_0 W_{in} L_{de}/d^2$ or $-3\mu_0 W_{in}^2/(U_{in}d)$. The comparison would invite us to state that inertial effects dominate viscous effects when $R_t > 6$. As a matter of fact, in the Berman problem (see below) the threshold of this event arises at $R_t^{iso} \approx 1.3107$.

Number λ is the channel length divided by the dead-end length. At first glance, condition $\lambda \ll 1$ should prevent the actual flow from axial flow exhaustion.

The significance of the number α becomes clearer when we compare the viscous pressure drop arising at the point of isobaric exhaustion with the inlet pressure. As a result, the ratio of $-3\mu_0 W_{in}^2/(U_{in}d)$ to P_{in} gives α^2. If $\alpha \geqslant O(1)$, viscous pressure drop is expected to have a serious influence on suction intensity. The reason why we choose α instead of α^2 will appear later, when the Regirer theory will be described.

As for number β, the reduced wall conductance, it is interpreted from the study of the flow inside the wall. Assume the Darcy law governs the transverse flow inside the wall of thickness e. It relates pressure drop to superficial velocity, and obviously gives

$$P_c(z) = \mu_0 e U_c(z)/K_D \qquad \text{which leads to} \qquad I_0 = \mu_0 e/K_D, \tag{2.6}$$

where K_D is the Darcy permeability, which has an order of magnitude related to the pore sectional area. This rough approach allows us to estimate number β as

$$\beta \equiv \mu_0/(I_0 d) = K_D/(ed). \tag{2.7}$$

Hence, it is evident that β is a very small quantity in most filtration processes.

Note that other authors use the longitudinal Reynolds number (or filtration Reynolds number), defined by $R_l = \rho_0 W_{in} d/\mu_0$. It reads $R_l = R_t\alpha/\sqrt{\beta}$ here.

Let us turn now to the dimensionless form of the Navier–Stokes equations. Applying change of unknowns and variables (2.4) and introducing numbers (2.5) we have to solve the following non-dimensional system in $\omega = \{0 < x < 1\} \times \{0 < z < \lambda\}$; domain ω now accounts for the plane of symmetry hypothesis

$$u_x + w_z = 0, \tag{2.8}$$

$$-p_x = \beta D_{[u,w;R_t,\beta/\alpha^2]}(u), \tag{2.9}$$

$$-p_z = \alpha^2 D_{[u,w;R_t,\beta/\alpha^2]}(w), \tag{2.10}$$

where $D_{[u,w;R_t,\beta/\alpha^2]}$ is the differential operator (acting below on the scalar function ϕ)

$$D_{[u,w;R_t,\beta/\alpha^2]}(\phi) = R_t(u\phi_x + w\phi_z) - (\phi_{xx} + \beta\phi_{zz}/\alpha^2). \tag{2.11}$$

The former boundary conditions now become in non-dimensional form

$$u(0,z) = 0, \quad u(1,z) = p(1,z), \quad w_x(0,z) = 0, \quad w(1,z) = 0. \tag{2.12}$$

A straightforward consequence of (2.9)–(2.11) can be established having in mind that u and w possess the same magnitude in non-dimensional form, as well as their different variations. Therefore, we can state in some norm, denoted $\|\,\|$,

$$\|p_x\| \approx \beta \|p_z\|/\alpha^2. \tag{2.13}$$

Consequently, Prandtl approximations are valid in the limit $(R_t/R_l) \longrightarrow 0$ (i.e. $\beta = 0$ and non-vanishing α). In this case, λ becomes a parameter of secondary importance: λ must be large enough to observe the predicted events (§ 5).

Another consequence can be derived from (2.8). Let us define $q(z)$, the non-dimensional mean axial velocity (or normalized flowrate) by $q(z) = \int_0^1 w(x, z)\,\mathrm{d}x$. Accordingly with the selected normalization, we have $q(0) = 1$. Performing the transverse partial integration of mass conservation law (2.8), we obtain

$$q'(z) \equiv \int_0^1 w_z(x, z)\,\mathrm{d}x = -\int_0^1 u_x(x, z)\,\mathrm{d}x = -[u]_0^1 = -u_c(z) = -p_c(z). \tag{2.14}$$

Hence, the variation rate of the mean velocity is equal to the pressure at the wall.

Let us now come to the linear theory of Regirer (1960) which is concerned with the particular case $\{R_t = 0, \beta = 0\}$ and looks for a solution with separation of variables. Thus, Regirer postulates $p(x, z) = p_c(z)$ (invoking the Prandtl approximation) and $w(x, z) = q(z)\theta(x)$. Reported in (2.10), and after elementary calculus, these hypotheses give

$$\theta(x) = 3(1 - x^2)/2 \quad \text{together with} \quad -p_c' = 3\alpha^2 q. \tag{2.15}$$

After eliminating pressure at the wall, we obtain the Regirer equation

$$q'' - 3\alpha^2 q = 0. \tag{2.16}$$

For given inlet pressure and flowrate $\{$i.e. $q(0) = 1$ and $q'(0) = -1\}$, the Regirer equation leads us to the following exact solution of the Navier–Stokes equations in $0 \leqslant z \leqslant \lambda$

$$q(z) = \cosh(\alpha z\sqrt{3}) - (\alpha\sqrt{3})^{-1}\sinh(\alpha z\sqrt{3}), \tag{2.17}$$

$$p(z) = -q'(z) = -\alpha\sqrt{3}\sinh(\alpha z\sqrt{3}) + \cosh(\alpha z\sqrt{3}). \tag{2.18}$$

The purpose of the next two sections is to provide us with ordinary differential equations (ODE) that extend the Regirer equation (2.16) to $R_t \neq 0$.

3. The Berman problem revisited

The Berman problem consists of a channel flow with a uniform crossflow (i.e. pressure-independent transpiration). In this section, it is set $u(1, z) = 1, \forall z$ (for an extension to more elaborate boundary conditions at a porous wall, see Chellam & Liu 2006). In consequence, $\hat{z}_{AFE}$, the distance of axial flow exhaustion (AFE) (i.e. $q(z = \hat{z}_{AFE}) = 0$), is easily found from mass conservation law. This event occurs at $\hat{z}_{AFE} = 1$ exactly. This is the reason why Berman proposed to search for an exact solution with a stream function (denoted $\psi(x, z)$) and the related velocities in the form

$$\psi(x, z) = (1 - z)B(x), \quad u \equiv -\psi_z = B(x), \quad w \equiv \psi_x = (1 - z)B'(x). \tag{3.1}$$

Substituted into equations (2.9)–(2.10), this hypothesis gives

$$-p_x = \beta[R_t BB' - B''], \tag{3.2}$$

$$-p_z = \alpha^2[R_t(BB'' - B'^2) - B'''], \tag{3.3}$$

while mass conservation law (2.8) is satisfied automatically. From (3.2), we obtain $p_{xz} = 0$, and deduce that the right-hand side of (3.3) is constant. More precisely,

Berman obtained the following ordinary differential equation,

$$R_t(BB'' - B'^2) - B''' = K(R_t) \quad \text{in } 0 < x < 1, \tag{3.4}$$

where constant $K(R_t)$, the so-called Berman's constant, is an unknown to be calculated from the boundary conditions in excess. Note from (3.3) that $-\alpha^2 K(R_t)$ gives the axial pressure variation. From (3.1), the boundary conditions imposed on ODE (3.4) are

$$B(0) = 0, \quad B''(0) = 0, \quad B(1) = 1, \quad B'(1) = 0. \tag{3.5}$$

The literature proposes powerful numerical methods (e.g. see Terrill 1964) for tabulating the solution of the Berman problem (3.4) complemented by four boundary conditions (3.5). One can claim that a 6-digit precision is easily obtained with 500 equidistant nodes in interval $0 < x < 1$. It has been shown that the solution is unique in the range of R_t concerned (more precisely, the Berman problem has a unique solution if $R_t < 12.165$), which can easily be approximated by an analytic expansion of the solution in a series of R_t (Terrill & Shrestha 1965; Rudraiah & Dinesh 2004; for recent developments of the method). Thus, these authors write the unknowns as

$$B(x) \equiv F(x; R_t) \equiv \sum_{n=0}^{n=\infty} \frac{1}{n!}\ f_n(x)\ R_t^n, \quad K(R_t) = \sum_{n=0}^{n=\infty} \frac{1}{n!}\ k_n\ R_t^n. \tag{3.6}$$

Then, substituting expansions (3.6) into ODE (3.4), and since ODE (3.4) is valid for every R_t, we obtain the following cascade of trivial differential equations

$$f_0''' = -k_0, \tag{3.7}$$

$$f_1''' = f_0 f_0'' - f_0'^2 - k_1, \tag{3.8}$$

$$f_n''' = n! \sum_{j=0}^{j=n-1} [j!(n-1-j)!]^{-1} [f_j f''_{n-1-j} - f'_j f'_{n-1-j}] - k_n, \ n > 1. \tag{3.9}$$

The use of symbolic calculus makes the integration of (3.7)–(3.9) straightforward. In a limited range of R_t (say $-4 \leqslant R_t \leqslant 4$), both series (3.6) are rapidly convergent. We define the approximate Berman's constant truncated at order N as $K(R_t; N) \equiv \sum_{n=0}^{n=N} (n!)^{-1}\ k_n\ R_t^n$. To fix the idea about the accuracy of this development, below we report $R_t^{iso}(N)$, the critical value of R_t that renders the flow isobaric (i.e. $K(R_t^{iso}(N); N) = 0$). We find

$$R_t^{iso}(N=1) = 1.29630, \quad R_t^{iso}(N=2) = 1.31101, \quad R_t^{iso}(N=3) = 1.31075,$$

while the 5-digit precision numerical computation gives $R_t^{iso}(Num.) = 1.31067$. Lastly, let us write the terms of the series up to $N = 2$.

$$f_0 = \frac{3x}{2}\left(1 - \frac{x^2}{3}\right), \quad k_0 = 3, \tag{3.10}$$

$$f_1 = \frac{x}{280}(-x^6 + 3x^2 - 2), \quad k_1 = -\frac{81}{35}, \tag{3.11}$$

$$f_2 = \frac{3x}{140}\left(\frac{x^{10}}{990} - \frac{x^8}{36} + \frac{x^6}{70} + \frac{73x^2}{1155} - \frac{703}{13860}\right), \quad k_2 = \frac{468}{13475}. \tag{3.12}$$

These data substituted in the different truncations of expansions (3.6) will provide us with the inlet boundary conditions consistent with the approximate solutions we shall derive in the next part. For moderate R_t, note furthermore that these profiles

correspond to slight (but not negligible) deviations from Hagen–Poiseuille flow, the latter being indeed the limit of either Berman flow for $R_t \to 0$, or Regirer flow for $\alpha \to 0$.

4. Analysis of channel flow with pressure-dependent suction

We now come to our original problem. Here, we set $u(x=1, z) = p(x=1, z), \forall z$. We shall take profit of the fact that the Berman solution is valid for any channel length (as soon as the entry conditions are of Berman type). In other words, between an entry located at z and an output at $z + \mathrm{d}z$, the Berman solution could hold for $r(z)$, the local transverse Reynolds number, defined as $r(z) = \rho_0 U_c(z) d/\mu_0$, or $r(z) = p_c(z)\rho_0 P_{in} d/(I_0\mu_0) = -q'(z)R_t$. Thus, let us look for a solution belonging to the class of the streamfunctions that satisfies the following form of variable separation:

$$\psi(x, z) = q(z)F(x; r(z)) \qquad \text{with} \qquad r(z) = p_c(z)R_t = -q'(z)R_t, \tag{4.1}$$

where the transverse flow profile $F(x; r)$ is the Berman solution (3.6) obtained with the local transverse Reynolds number $r(z) = -q'(z)R_t$. The velocity components become

$$u(x, z) \equiv -\psi_z = -q' F + R_t q q'' F_r, \quad w(x, z) \equiv \psi_x = q F_x. \tag{4.2}$$

We easily confirm that $q(z)$ is the normalized flowrate (or mean velocity), and that the pressure-dependent boundary condition is plainly satisfied, since $u(x=1, z) = -q'(z) = p_c(z)$. Substituting expressions (4.2) into the Navier–Stokes equation (2.10), we obtain

$$p_z = \alpha^2 q \left\{ K[r(z)] + R_t^2 q q'' [F_r F_{xx} - F_x F_{xr}] \right\} - \beta E(x, z), \tag{4.3}$$

where the differential expression $E(x, z)$ is given by

$$E(x, z) = q'' F_x - R_t [2q'q'' - qq''']F_{xr} + R_t^2 q q''^2 F_{xrr}. \tag{4.4}$$

From PDE (4.3), the validity of which is extended to $x = 1$, we establish

$$p_z(x = 1, z) \equiv -p_c'(z) = \alpha^2 q K[r(z)], \tag{4.5}$$

since other terms of (4.3) obviously vanish at $x = 1$. A particularly interesting differential expression on q can now be obtained after eliminating p_c between (2.14) and (4.5)

$$q'' = \alpha^2 q K[-R_t q'(z)] \quad \text{or} \quad q'' = \alpha^2 q \sum_{n=0}^{n=\infty} (n!)^{-1} k_n (-q')^n R_t^n. \tag{4.6}$$

Let us now consider the conditions that render a truncation of differential expression (4.6) (i.e. an ODE) equivalent to Navier–Stokes equations. Inspection of PDE (4.3) indicates that the condition $\beta = 0$ allows us to cancel the x-dependence contained in $E(x, z)$, and furthermore makes the pressure independent of x (i.e. $p(x, z) = p_c(z) = -q'(z)$). The only remaining x-dependence is in $(F_r F_{xx} - F_x F_{xr})$, evidently pushed away to the second order in R_t. Consequently, if we restrict the expansion in R_t to zero and first orders, PDE (4.3) degenerates (if $\beta = 0$) into the following two ODEs

$$q'' = \alpha^2 q \sum_{n=0}^{n=N} (n!)^{-1} k_n (-q')^n R_t^n, \quad \text{for } N = 0, N = 1. \tag{4.7}$$

The ODE for $N=0$ is nothing but the Regirer equation (2.16), while the ODE for $N=1$ is new. The latter reads

$$q'' = \alpha^2 q(k_0 - k_1 R_t q'). \tag{4.8}$$

It is worthy of note that Galowin *et al.* (1974) endeavoured to take account of inertial effects within Regirer theory; by assuming a Hagen–Poiseuille profile all along the duct and integrating on the transverse coordinate, they obtained an ODE of the same form as ODE (4.8). As a result, the present theory shows that their derivation is, however, not consistent with the spirit of a development at the first order in R_t, since their procedure would find for a two-dimensional channel the value $-12/5$ in place of k_1 ($k_1 = -81/35$). It is nevertheless noticeable that the discrepancy between their heuristic approach and the present one is quite small (only a 5 % error).

Lastly, we inspect what happens at the second order in PDE (4.3), i.e. we now envisage extending ODEs (4.7) to $N=2$. At the second order, PDE (4.3) becomes

$$q''\left(1 - g_0(x)\alpha^2 R_t^2 q^2\right) = k_0\alpha^2 q\left(1 - \frac{k_1}{k_0}R_t q' + \frac{k_2}{2k_0}R_t^2 q'^2\right), \tag{4.9}$$

where $g_0(x) \equiv f_1 f_0'' - f_1' f_0' = [-15x^8 + 21x^6 + 9x^4 - 21x^2 + 6]/560$. Evidently, the second-order expression (4.9) is not a true ODE. However, the departure from an ODE remains small because, as long as $\alpha^2 R_t^2 \approx O(1)$, the quantity $\|g_0\|_\infty \approx 10^{-2}$ has always to be compared with 1 (whereas this rationale is not valid for the second-order term in the right-hand side of (4.9)). Therefore, under those conditions, we stress the fact that the ODE,

$$q'' = k_0\alpha^2 q\left(1 - \frac{k_1}{k_0}R_t q' + \frac{k_2}{2k_0}R_t^2 q'^2\right), \tag{4.10}$$

is able to govern the flowrate in the duct within a few per cent accuracy. Note, finally, ODE (4.10) is nothing more than differential expression (4.6) truncated after the term $n=2$. Next, we present an application of the present analysis for moderate R_t.

5. Axial flow exhaustion (AFE) *vs*. crossflow reversal (CFR)

In practice, the experiments in filtration are operated to prevent the membrane flow from two unwanted events. On the one hand, too long a channel leads to the extinction of the axial flow: this event – called 'axial flow exhaustion' (AFE) already – arises at the exhaustion length, noted $\hat{z}_{AFE}$ (and measured in units of dead-end length $L_{de} = W_{in}d/U_{in}$). On the other hand, a long enough channel experiences a strong viscous drop of the membrane inner pressure: if the inner pressure becomes lower than the external pressure, suction stops, and injection takes place. In other words, a 'crossflow reversal' (CFR) can arise at a distance called $\hat{z}_{CFR}$ hereinafter (in capillary flow, $\hat{z}_{CFR}$ might be interpreted as the locus where the transition from arterial system to venous side occurs). Parameter λ is now assumed large enough to permit the occurrence of these events.

For $R_t = 0$, the Regirer solution (2.17)–(2.18) predicts

$$\hat{z}_{AFE} = (\alpha\sqrt{3})^{-1}\tanh^{-1}(\alpha\sqrt{3}), \quad \hat{z}_{CFR} = (\alpha\sqrt{3})^{-1}\tanh^{-1}[(\alpha\sqrt{3})^{-1}]. \tag{5.1}$$

If $\alpha < 1/\sqrt{3}$, $\hat{z}_{AFE}$ is greater than 1, and CFR never arises ($\hat{z}_{CFR}$ being not defined in (5.1)). In other words, AFE is the only dangerous event. Conversely, if $\alpha > 1/\sqrt{3}$, $\hat{z}_{CFR}$ is defined in (5.1). It is a decreasing function of α (from infinity to zero), while

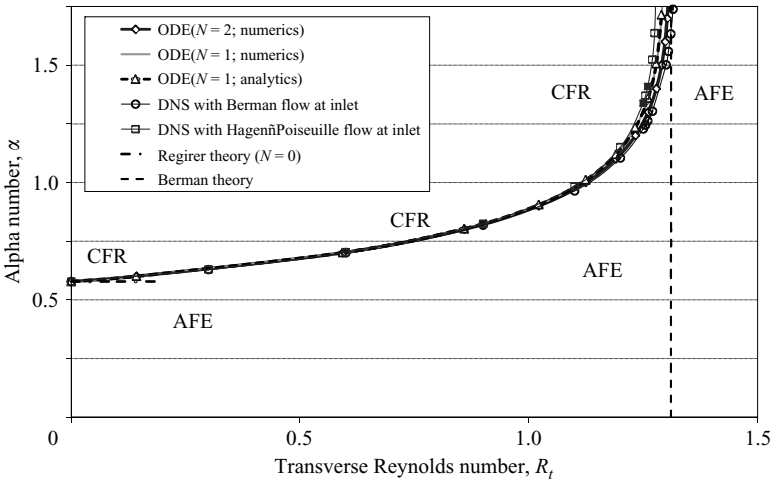

FIGURE 2. Respective domains where axial flow exhaustion (denoted AFE) or crossflow reversal (CFR) is the event that threatens filtration. Both domains are separated by a curve that joins point $\{R_t = 0, \alpha = 1/\sqrt{3}\}$ and point $\{R_t = R_t^{iso}, \alpha = \infty\}$. Four approximations of this curve are plotted; two results from the ODEs obtained for $N = 1$ and $N = 2$; the other two come from numerical simulations with different entry flows of Berman or Hagen–Poiseuille type.

the AFE event never occurs ($\hat{z}_{AFE}$ is not defined in (5.1)). In other words, CFR is now the event that threatens the filtration process. For the particular value $\alpha = 1/\sqrt{3}$, Regirer (linear) theory predicts that $\hat{z}_{CFR} = \hat{z}_{AFE} = \infty$. In the latter case, the channel carries a vanishing flowrate up to infinity, as well as a vanishing suction.

On the other hand, isobaric flow (obtained for $R_t = R_t^{iso} \approx 1.3107$ after Berman theory) has the exhaustion length $\hat{z}_{AFE} = 1$. In accordance with (3.3)–(3.4), isobaric flow requires $K(R_t) = 0$ (provided that $\alpha^2 \neq \infty$). Of course, CFR never occurs for finite α^2.

Let us now consider in the diagram $\{R_t, \alpha\}$ (figure 2), the occurrence domains of AFE or CFR. Both domains are expected to be separated by a curve, the locus where both events occur at the same distance from the inlet (i.e. $\hat{z}_{CFR} = \hat{z}_{AFE}$). In figure 2, the point $\{R_t = 0, \alpha = 1/\sqrt{3}\}$ stands on this separation curve. The line $R_t = R_t^{iso}$ is entirely situated in the AFE domain, except for the point $\{R_t = R_t^{iso}, \alpha = \infty\}$ which stands on the separation curve, too. This is because – for very large α – the flow experiences an unlimited pressure drop even in the vicinity of $R_t = R_t^{iso}$. This leads to the appearance of CFR.

The next problem is to find the separation curve, or how to connect the latter points in this diagram. The use of the new ODEs will allow us to shed light on this issue.

For simplicity, let us rewrite (4.8) as

$$q'' = aq\left(1 + bq'\right) \quad \text{with} \quad a = k_0\alpha^2, \quad b = -k_1 R_t / k_0. \tag{5.2}$$

As suggested by the discussion above, the curve searched for is situated in the domain $0 \leqslant b < 1$. Therefore, $p = -q'$ being smaller than one from inlet to $\hat{z}_{CFR}$, the following change of unknown is meaningful

$$y = \ln(1 + bq'). \tag{5.3}$$

Substituted in ODE (5.2), this leads to the new form

$$y''-a\,\{(\exp(y)-1\}=0 \quad \text{with the boundary conditions} \quad y(0)=\ln(1-b), \quad y'(0)=ab \tag{5.4}$$

This new ODE has the advantage of leading to the following integrated form

$$y'^2/(2a)=ab^2/2+\exp(y)-(1-b)-[y-\ln(1-b)]. \tag{5.5}$$

By imposing simultaneously both conditions of AFE ($y'=0$, i.e. $q=0$) and CFR ($y=0$, i.e. $q'=0$) on expression (5.5), we obtain the equation of the curve sought for

$$a=\frac{2}{b^2}\,[-\ln(1-b)-b] \quad \text{or} \quad \alpha=\frac{k_0\sqrt{2}}{|k_1|R_t}\left[-\ln\left(1-\frac{k_1}{k_0}R_t\right)-\frac{k_1}{k_0}R_t\right]^{1/2}. \tag{5.6}$$

Figure 2 shows several approximations of the separation curve. Two of them results from both ODEs (i.e. for $N=1, 2$). The first one (relative to the ODE obtained with $N=1$) is drawn from analytical expression (5.6) for values up to $R_t=-k_0/k_1$. This curve is complemented with results from the numerical integration of ODE (4.8) for R_t values higher than $-k_0/k_1$. The second separation curve plotted in figure 2 comes from the numerical integration of ODE (4.10) (i.e. the ODE obtained with $N=2$). As expected, it is worth observing that the second-order ODE gives better precision at high R_t, since the resulting separation curve admits the line $R_t=R_t^{iso}$ as asymptote. The second-order ODE (4.10) nearly perfectly performs the junction between points $\{R_t=0, \alpha=1/\sqrt{3}\}$ and $\{R_t\approx 1.3107, \alpha=\infty\}$.

Lastly, numerical computations of the Navier–Stokes equations (NSE) have been carried out within the context of the Prandtl approximation ($\beta=0$). More details about the numerical method will be given elsewhere. This approach allows us to determine numerically the separation curve. Two kinds of results are presented in figure 2. The first one corresponds to NSE computed with Berman inlet conditions; as expected, the resulting separation curve almost coincides with the curve labelled ODE ($N=2$). As for the second numerical result, it is concerned with NSE computations with Hagen–Poiseuille inlet conditions; we observe that the slight discrepancy with ODE ($N=2$) occurring at $R_t>1$ remains acceptable. In other words, the present theory advances predictions that are also useful for entrance conditions more standard than those of the Berman type.

To sum up, for small and moderate transverse Reynolds numbers, we have proposed two new ODEs, (4.8) and (4.10), valid for vanishing β. They are intended to partly fill the gap between Berman and Regirer theories in the range $0\leqslant R_t\leqslant 4$, which is supposed to include the standard operational domain in filtration. The present approximate approach should correspond to the analytical work that has often been requested by experimentalists: e.g. Mellis, Gill & Belfort (1993) found that the Berman and Regirer theories were unable to account for their experiments at $R_t>0.5$.

The author thanks Professors F. Charbit and P. Guichardon for encouragement and enlightening discussions.

REFERENCES

Bacchin, P., Aimar, P. & Field, R. W. 2006 Critical and sustainable fluxes: theory, experiments and applications. *J. Membrane Sci.* **281**, 42–69.

Berman, A. S. 1953 Laminar flow in channels with porous walls. *J. Appl. Phys.* **24**, 1232–1235.

Brady, J. F. 1984 Flow development in a porous channel and tube. *Phys. Fluids* **27**, 1061–1067.

Chellam, S. & Liu, M. 2006 Effect of slip on existence, uniqueness, and behavior of similarity solutions for steady incompressible laminar flow in porous tubes and channels. *Phys. Fluids* **18**, 083601.

Galowin, L. S., Fletcher, L. S. & DeSantis, M. J. 1974 Investigation of laminar flow in a porous pipe with variable wall suction. *AIAA J.* **12**, 1585–1589.

Gupta, B. K. & Levy, E. K. 1976 Symmetrical laminar channel flow with wall suction. *Trans. ASME* I: *J. Fluids Engng* **33**, 469–475.

Mellis, R., Gill, W. N. & Belfort, G. 1993 Fluid dynamics in tubular membrane: theory and experiments. *Chem. Engng Commun.* **122**, 103–125.

Regirer, S. A. 1960 On an approximate theory of viscous incompressible fluid flow in channels with permeable walls. *J. Tech. Phys. (Zh. Tekh. Fiz.)* **30**, 639–643.

Robinson, W. A. 1976 Existence of multiple solutions for laminar-flow in a uniformly porous channel with suction at both walls. *J. Engng Maths* **10**, 23–40.

Rudraiah, N. & Dinesh, P. A. 2004 Nonlinear flow between permeable disks using computer extended series method. *Stud. Appl. Maths* **113**, 163–182.

Terrill, R. M. 1964 Laminar flow in a uniformly porous channel. *Aeronaut. Q.* **15**, 299–310.

Terrill, R. M. & Shrestha, G. M. 1965 Laminar flow through parallel and uniformly porous walls of different permeability. *Z. Angew. Math. Phys.* **16**, 470–482.

Zaturska, M. B., Drazin, P. G. & Banks, W. H. H. 1988 On the flow of a viscous fluid driven along a channel by suction at porous walls. *Fluid Dyn. Res.* **4**, 151.